Automated segmentation of bone with single zero-echo time imaging

Sandeep Kaushik[1], Dattesh Shanbhag[1], and Florian Wiesinger[2]
[1]*GE Global Research, Bangalore, Karnataka, India,* [2]*GE Global Research, Munich, Germany*

Target Audience: Researchers interested in obtaining bone structure from MRI data

Introduction: In the recent times, interest in using MR for bone imaging has significantly increased. MR bone imaging finds utility in interventional applications like MR-based attenuation correction in PET/MR and MR-based radiation therapy planning. Accurate depiction of bone structures using MR is particularly challenging due to low proton density (PD) and very quick signal decay. Bone imaging with ultra-short TE pulse sequences achieve selective bone depiction by dual echo acquisition and subtracting the longer echo from shorter echo to retain only short T2 tissue structures. However, this results in a longer scan time. Zero echo time pulse sequence (ZTE) provides mechanism to depict bone in MRI [1]. In ZTE, low flip angle provides PD-weighted contrast, and high bandwidth (BW=±125kHz) acquisition provides efficient sampling of short T2 structures and also results in fast scanning with sub-millisecond TR. In this work, we present a novel method for efficient segmentation of bone in head ZTE images, using a single TE, complex MRI data along with histogram-based RF intensity correction method.

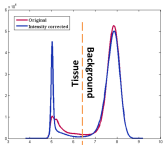

***Fig.1**: Histogram of log-transformed magnitude ZTE data*

Methods and Materials: **Zero TE imaging**: Three volunteer images were acquired using ZTE pulse sequence in a GE 3T MR750w scanner, equipped with a GEM HNU NV receive array (GE Healthcare, Waukesha, WI). ZTE parameters were: FOV=32cm, res=1.25 mm, FA=1.2°, 256x256x256 matrix. The studies were approved by the appropriate IRB. Complex MRI images were reconstructed and are represented in analysis as: $I(r, \theta) = r*\exp(i\theta)$, with r being the magnitude and θ being the phase.

***Fig.2**: Intensity corrected images*

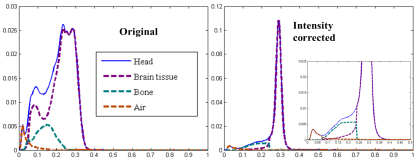

***Fig.3**: 3-class histogram of original **(L)**; and intensity corrected **(R)** magnitude ZTE images (bone /air distribution magnified in the inset).*

Histogram-based intensity correction: As a preprocessing step to segmentation, a histogram-based RF intensity correction was developed which takes advantage of the flat, non-contrast characteristic of PD-weighted ZTE images. Due to PD contrast, image histogram of the log-scaled ZTE image (Fig.1) contains primarily two peaks (brain and background). From the histogram, the SNR and full-width-half-maximum (FWHM) of the two peaks can be estimated. The soft-tissue peak is broadened by the spatially non-uniform transmit and receive sensitivities. In a smaller region-of-interest (ROI) with less variation of the sensitivity profiles, the signal peak becomes significantly narrower and the soft tissue signal in this ROI can be approximated by the location of the signal peak. Based on this observation, bias correction together with signal normalization was accomplished within iterative multi-resolution approach by i) dividing the 3D image dataset into ROIs and ii) normalizing all pixels within a certain ROI by the peak maximum of the corresponding soft tissue peak. The estimated bias field is Gaussian smoothened to eliminate the checkerboard pattern from the discrete ROIs and applied on original ZTE image. **Phase alignment**: Using pre-segmented regions of 4-classes (background, air in head, tissue and bone) in one of the data, histogram of the phase in each class was studied to understand their distribution and relative positioning. We observed that phase in air class has overlap with other tissues (white noise), with peak being distinctly separated (Fig 4a). Therefore to reduce the overlap of air phase with other tissues, we tilted the air signal vectors away from the bone and tissue signal vector by 180°. This was accomplished as: $I_{bias}(r,\theta) = \alpha*\sigma_{air}*\exp(i(\pi+\mu_{\theta sig})) + I(r,\theta)$. Here α is a scaling factor, σ_{air} is the standard deviation of air regions and $\mu_{\theta sig}$ is the average signal phase. **Segmentation:** The goal of segmentation is to classify the ZTE image into three classes – soft tissue, bone and air. The intensity corrected ZTE magnitude data, by aforementioned method, is first segmented into body mask, air mask (typically sinuses are segmented) and background regions (Fig.5b) using the phase-field segmentation method [2]. Within the body region, log transformation is applied to enhance the bone structures and air regions against the soft tissue (Fig.5c). In order to segment the three classes within the body region, a multi-pass, multi-level threshold scheme is introduced on log transformed data using maximum entropy metric [3]. In the first pass of segmentation, a four class threshold yields the labels as: ***label 1*** = tissue + vertebrae**,** ***label 2*** = bone, ***label 3*** = air and ***label 4*** = petrous bone mixed with air (Fig.5d). We observed that the air voxels at the rim of the body mask have similar intensity to bone voxels and are captured as bone label (*label 2*) (Fig.5e). To remove the surface air voxels, an approximate signed distance transform [4] is applied to the body mask and a threshold of 5mm used to identify the air exclusion zone. Similarly, we applied the signed distance transform to the internal air-mask and identified an exclusion zone around it as well. Once the air is excluded, *label=2* in first pass threshold primarily captures the skull. Next, we mask out the voxels with labels = 2, 3 and 4 in the log transformed ZTE data and perform second round of 4-class threshold on the masked data. This allows the soft tissue and vertebrae classes to be separated. The output of second pass threshold mask would contain mixed labels of air in regions around trachea and these are cleaned up using air exclusion zone. A connected component analysis is performed to retain the largest connected component which is the skull and vertebrae (Fig.5f). In order to refine the air and ambiguous regions of air and petrous bone (labels = 3,4), phase information is used. It is observed from the histogram of phase data (Fig. 4 a , b), that air phase has more variance than soft tissue and bone phase (Fig 4a,b, jitter in air histogram). A standard deviation (SD) map of phase data was therefore constructed (Fig 5a). A Gaussian curve was fit around the largest peak of the SD map histogram (mostly tissue and bone voxels) and mean and SD calculated (μ_{std}, σ_{std}). Air voxels were identified by setting a threshold > $\mu_{std}+3*\sigma_{std}$ (Fig.5b). The air regions so obtained were merged with label = 3. A final three class mask is obtained by combining the refined regions of: soft tissue region, bone+ vertebrae and air.

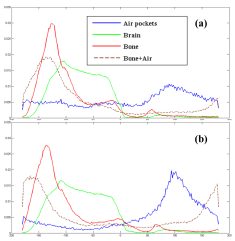

***Fig.4**: Phase distribution in different classes **(a)** before and **(b)** after intensity correction*

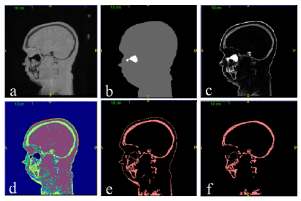

***Fig.5**: **(a)** - **(f)** Different stages of segmentation on magnitude images*

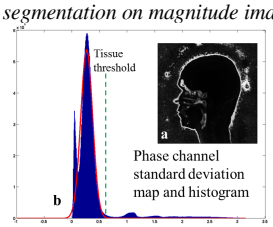

***Fig.6**: (**a**) SD map of aligned phase data and (**b**) its histogram show air regions to be of most varying phase.*

Results and discussion: The intensity correction method removes the RF shading significantly and provides an uniform image for segmentation (Fig.2). The sharpened histogram for tissue class post intensity corerction allows reliable seperation of soft tissue from bone and air using magnitude only data (Fig.3). Maximum entropy based multi-level thresholding and subsequent two-pass processing provides reliable segmentation of skull and vertebrae (Fig. 5). However, magnitude only data cannot resolve the amiguity in air and hard petrous bone. The air phase alignment method tilts the general phase of air regions away from other tissue classes and enables reliable air segmentation by threshold of the phase data (Fig. 6). This also achieves seperation of air from petrous bone. Overall, use of complex MRI data allows excellent depiction of bone and vertebrae structres from ZTE MRI images (Fig 7 and 8). We noticed that some regions at the base of ZTE images are classified as bone due to these regions being outside of coil coverage and poor SNR and can be addressed by aquiring images in shorter FOV.

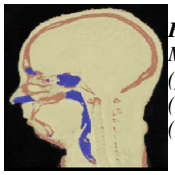

***Fig.7**: (**a**) Final Mask of Tissue (yellow), bone (orange) and air (blue)*

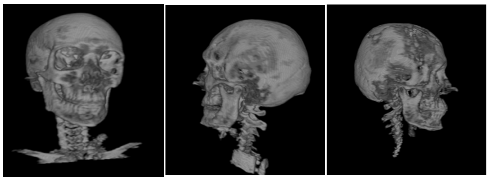

Fig.8. Bone segmentation in head with complex ZTE-MRI data in three cases. Notice excellent depiction of skull, vertebrae and teeth.

Conclusion: Excellent 3D cortical bone depiction in the head was achieved using single-echo, dual channel ultra-short TE imaging in combination with RF intensity correction and an inverse logarithmic image scaling (Fig.8). As a next step, the performance of the presented method needs to be evaluated against a ground truth from CT images.

References: **[1].** F. Wiesinger, et al., ISMRMB 2013 **[2].** Shanbhag et.al. 20th ISMRM 2012, p.437; **[3].** J. Kapur, et al., Comput. Vis. Graph. Image Process. vol.29, p.273–285; **[4].** ITK ApproximateSignedDistanceMapImageFilter